Journal of Advances and Scholarly Researches in Allied Education
Vol. 20, Issue No. 2, April-2023, ISSN 2230-7540

Nanostructured Solar Cell Performance in Relation to the Anodic Aluminum Oxide Membrane

Narendra Kumar[1]*, Dr. Ravi Shankar Kumar[2]

[1] Research Scholar, S.K.M. University, Dumka

[2] Assistant Professor, S.P. College, Dumka

Abstract - To illustrate how the host anodized aluminum oxide (AAO) membrane influences device performance, three different nanowire solar cell designs have been constructed. The comparable transmittance spectra amongst the three arrangements suggest that the AAO membrane has very low optical absorption. The device's power conversion efficiency (PCE) is investigated, and compared across cell topologies with and without an AAO membrane, as a function of carrier transit and collection. Nanowire solar cells can stand on their own and have a PCE of 9.9%. PCE is increased to 11.1%-11.3% by including AAO into the solar cell structure, which reduces interface defects and traps brought on by humidity and oxygen, and stops CdTe tentacles from coming into direct touch with SnO2 and forming micro shunt shorts. Partially embedded nanowire solar cells are a desirable construction because they create a high number of carriers in the axial direction and a relatively low number of carriers in the lateral direction, mitigating the effects of non-ideal and non-uniform nanowire development. As a result, the incorporation of an AAO membrane into the design of a solar cell results in improved electro-optical and mechanical characteristics.

Keywords - nanowire solar cells, cadmium sulfide nanowires, AAO membrane patterning

----------X----------

INTRODUCTION

There has been a lot of research on nano porous anodic alumina (NAA) during the last two decades. Since the development of the two-step anodization technique by Masuda et al.,1-3 NAA has found applications across a wide range of scientific disciplines thanks to its ability to fabricate highly ordered holes at the nanoscopic scale. In fact, they are very versatile because of their capacity to be fabricated into layers or laminas with holes of varying thicknesses, sizes, and interpore distances. Many different areas of study have taken use of NAA so far, including optical sensors biosensors cell culture drug delivery crystallization enclosures and energy storage Included in the other gadgets. However, NAA still has a problem with ohmic contact between the material infiltrated in the holes and the substrate being impossible due to the existence of an insulating barrier layer oxide at the bottom of the pores. Because the materials infiltrating the NAA layer would need to be electrically coupled to the aluminum electrode, its use in energy storage devices (batteries, supercapacitors), energy generating devices (photovoltaic cells), and electrical sensors has been restricted.

Researchers have developed methods that include many rounds of reanodization and chemical etching to mitigate some of these drawbacks. However, these methods may be time-consuming and often fail to completely remove the barrier layer. Methods such as incremental voltage stepdown, incremental current stepdown, constant current consecutive reanodization, and cathodic polarization are used during reanodization in sulfuric or oxalic acid. With interpore lengths greater than 300 nm after moderate anodization, we have recently disclosed a method to selectively remove the barrier layer.35 By doing so, the barrier layer may be eliminated entirely, and an ohmic contact can be established between the substance used to fill the pores and the aluminum substrate. Here, we describe a perovskite solar cell (PSC) in which the nanostructured alumina serves as an enclosure for the perovskite absorber layer (methylammonium lead iodide, MAPbI3) and the aluminum substrate serves as the cathode, in order to evaluate the viability of the aforementioned method for the production of devices in which an ohmic contact is required.

As has been shown in the past, the crystallization behavior of MAPbI3 is anticipated to be significantly affected by the confinement of the material in the pores. The encapsulation of the perovskite absorber has been shown to retard the diffusion of moisture through the active layer, leading to increased

stability in PSC devices where the absorber perovskite was partially infiltrated in a nano porous scaffold. Furthermore, it has been shown that organic compounds crystallize differently in nanoscopic enclosures than they do when crystallized in the open air. Therefore, crystallizations carried out in NAA holes often permit the production of polymorphs that would not be possible under normal conditions. They may modify the rate of crystal growth and cause the crystal to grow in a preferred direction of the lattice.

LITERATURE REVIEW

Abdelilah Slaoui, et.al (2020) In this chapter, we will cover the basics of how nanotechnology may be used to photovoltaics, including the key concepts, materials, and devices. We'll start with the basics of photovoltaics, including some of the underlying science and technology. In this way, we may design photovoltaic devices that are optimal for nanomaterials. In this article, we will go through the theoretical and experimental aspects of the geometrical (interpenetrating structures), electrical (work function), and optical (quantum confinement, photonics, plasmonic) effects of nanomaterials. Solar cell devices incorporating nanomaterials (including those based on ideas that exceed conventional cells in a variety of ways, etc.) will also be addressed, along with their features.

Gerrit Boschloo et.al (2019) Dye-based solar cells have been the subject of a great deal of research in the last three decades. However, there are many untapped possibilities for enhancing their efficacy that have yet to be investigated. Dye performance might benefit from continual experimentation with the molecules that make them up. For instance, inserting steric groups may slow down recombination processes and prevent unwanted aggregation. Dye packing on the mesoporous TiO2 surface might be optimized to better absorb and block light. Alternative redox pairs to the typical triiodide/iodide pair may produce substantially higher output voltage, making the adoption of innovative redox mediators and HTMs particularly advantageous for high-throughput oxidation-reduction (DSC) operations.

Karwan Wasman Qadir (2022) Plasmons may aid in the energy conversion process of DSCs when gold (Au) nanoparticles (NPs) are incorporated with Titania (TiO2) photoanodes. There is a need to improve DSSCs' energy conversion efficiency., PCE technology was augmented with gold nanoparticles (GNPs). The purpose of this research is to optimize DSSC performance by increasing optical absorption. Using finite-difference time-domain (FDTD) software, TiO2 photoanodes with GNPs of varying radii (15, 25, 35, 45, 55, 65, 75, and 85 nm) were created. Since plasmon coupling has a bigger impact on metal nanoparticles larger than 60 nm, we calculated that a radius of 85 nm is ideal for the enhancement of optical absorption. This study also demonstrates how the extent to which light is scattered varies with the size of the GNPs. TiO2 sheet absorbance as a function of incident angle has also been investigated. For maximum broadband optical absorption between 450 and 800 nm, an incidence angle of 70 degrees was found to be optimal.

William Ghann et.al (2018) As a result of the impact to investigate the impact of europium on the current and voltage characteristics of the DL680 dye sensitive solar cell, solar cells were fabricated using DyLight680 (DL680) dye and its equivalent europium conjugated dendrimer, DL680-Eu-G5PAMAM. We used a variety of spectroscopic techniques, such as absorption and emission spectroscopy, fluorescence lifetime, and Fourier transform infrared spectroscopy, to examine dye samples. It was also observed that titanium dioxide nanoparticles were sensitive to the DL680-Eu-G5PAMAM dye. transmission electron microscopy analysis of the dye and its molecular interaction with the nanoparticles. The New DL680-Eu-G5PAMAM Model When placed in direct sunshine (100 mWcm2, AM 1.5 Global), the electrical power output of dye-sensitized solar cells was 0.32 percentage points higher than that of DL680 cells. The enhanced performance might be attributed to europium, a chemical element that enhances a dye's ability to absorb sunlight.

Riya Datta et.al (2019) Rising power consumption, environmental concerns, and the fast advancement of associated technologies have opened up new opportunities for using renewable energy. Solar energy has the lowest conversion and maintenance losses, is consistently available, and has cheap costs. Solar photovoltaics are now the most used method of solar absorption. Solar cells' popularity as a renewable energy source has skyrocketed in recent years. In the nineteenth century, it was realized that solar energy could be harnessed to provide useable power, marking the beginning of the era of photovoltaic cells. Photovoltaic cells are a clean and sustainable way to generate power, and might one day make fossil fuels obsolete. The pressure to develop and capitalize on renewable energy sources at scale is on the rise. Combining nanoscale supported particles with semiconducting polymers has allowed for the development of solar cells with usable power conversion efficiency in recent years.

CHARACTERISTICS AND ANALYSIS OF THE NANOWIRE SOLAR CELL ARCHITECTURE

Scanning electron micrographs of three distinct CdS nanowire architectures, shown topically and laterally. It's possible that the nanowires' vertical orientation will be preserved after CdTe deposition. Crystalline CdS nanowires that have been partly exposed. Long-range, well-aligned, packed rows and columns describe all three geometric CdS nanowire forms. Predicted averages for length, diameter, and the distance between the centers of adjacent nanowires range from 100 nm to 60 nm to 106 nm. Therefore,

CdS nanowires should have a porosity of 32% and a density of 1.14 x 1010 nanowires/cm2. Nanowires presented here are able to preserve their nanowire structures even after many high-temperature annealing procedures, in contrast to nanocrystalline materials published elsewhere. To put it another way, an AAO membrane typically takes up just about 68% of the area of a device, whereas CdS nanowires take up only about 32%. Nanowires in this application are expected to exhibit visual and electrical differences due to the CdS window.

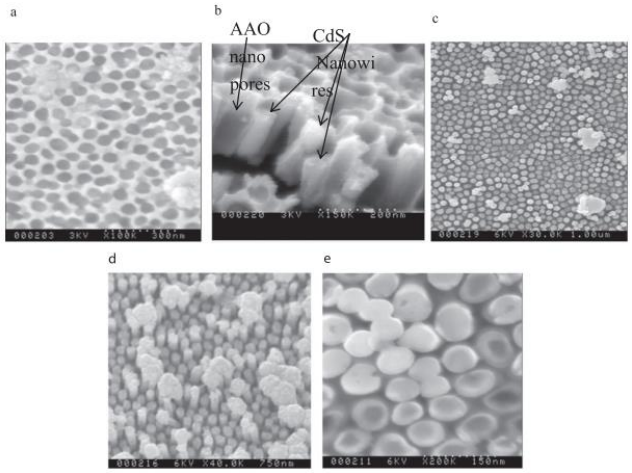

Figure 1: A SEM photo showing Both the top and bottom ends to the AAO membrane, the CdS nanowires got securely rooted. Top view (c) and cross-sectional (d) SEM images of CdS nanowires. The AAO membrane with inserted CdS nanowires, as shown by scanning electron microscopy (SEM)

CDS NANOWIRES WITH OPTIMAL GEOMETRICAL SHAPES

Power conversion must be optimized for Three-dimensional geometric CdS nanowire transmission must be characterized over a broad wavelength range (300-860nm), covering the entire visible light spectrum from NIR to the bandgap edge of the CdTe absorber, for a solar cell to function properly. light spectrum via the three angled cadmium selenide nanowires. The transmittance of fully embedded and partially embedded CdS nanowires is astonishingly close to that of free standing CdS nanowires across the wavelength range of 300 to 860 nm.

The low permeability of the AAO membrane is further supported by these results. Strong Three-geometric CdS nanowire transmission beginning at 350 nm demonstrates the widened bandgap of confined CdS nanowires in AAO nanopores. The AAO membrane takes up around 68% of the volume of the window layer, as shown in SEM images, while the CdS nanowires account for the remaining 32%. Since the effective energy band gap of CdS nanowires is larger than that of the AAO membrane, some of the incident light across the entire spectral range can pass directly through the absorption-negligible AAO membrane, while the other portion of the incident light transmits through the much less dense CdS nanowires.

Incoming photons will pass through the AAO membrane and be absorbed by the CdTe absorber in the freestanding CdS nanowires. Light is absorbed by the CdTe layer, making accessible a significantly brighter and wider range of incident light. In addition, the considerable front surface recombination loss is mitigated by the nanowire CdS window layer, which efficiently directs the wide-wavelength photons into the CdTe absorber. reason for device failure in nanostructure silicon photovoltaics. The CdS nanowires produced by AAO in the window layer improve light transmission by enhancing absorption of CdTe.

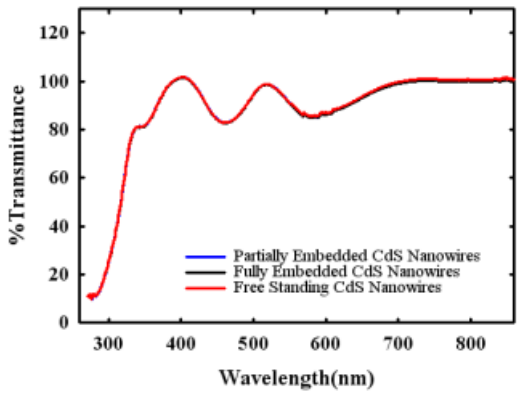

Figure 2: Transmission spectra for fully doped CdS nanowires embedded, partly embedded, and not embedded at all.

COMPARING THE J-V CURVES OF THREE DISTINCT CDS-CDTE SOLAR CELLS BASED ON THE GEOMETRY OF NANOWIRES.

Three geometric nanowire Solar cells were examined in both the dark and with 100mW/cm2 of light to investigate the impacts of interfaces generated between the AAO membrane and CdTe, which have a large influence on the photovoltaic properties. We dissect the J-V Plots and evaluate the differences and similarities between the three distinct varieties of geometric nanowire solar cells. Changes in the photoconductivity and space charge of CdS nanowires and CdTe during illumination may be directly ascribed to the observed transition from dark to lit states in the J-V curves of all three geometric nanowire solar cells. From dark JV curves, we may infer the diode quality factor (N) and the reverse saturation current density (Jo) to evaluate main junction performance. To account for the absence of series and shunt resistances, we use the slope and intercept of the dark ln(J)-V data obtained with a forward bias between 0.35 and 0.65V to determine the amount of nitrogen and jo recovered. N and Jo, determined using dark J-V observations, are shown in the table.

PENSCs can only reach 2.50 N efficiency and 6.32*108 Jo A/cm2, but free-standing PENSCs can reach 2.79 N efficiency and 1.19107 Jo A/cm2. The Jo values of fully embedded nanowire solar cells (FENSC) are somewhat higher than those of PENSC

(n = 2.53), at 6.45*108 A/cm2. Interface flaws, sometimes known as traps, and junction behavior are represented by the symbols N and Jo, respectively. Interface recombination and tunneling currents are induced when N and Jo are raised in free-standing nanowire solar cells, demonstrating a high density of interface defects and traps. Partially or totally submerged CdS nanowires protected by an AAO membrane significantly enhance the interface defects, traps, and junction behavior of nanowire solar cells. The Fill factor and Voc of the device benefit most from having low N and Jo values. Dark recombination current is decreased, and device performance is increased, thanks to the AAO membrane's enhanced interface and junction characteristics between the CdS nanowire and the CdTe layer.

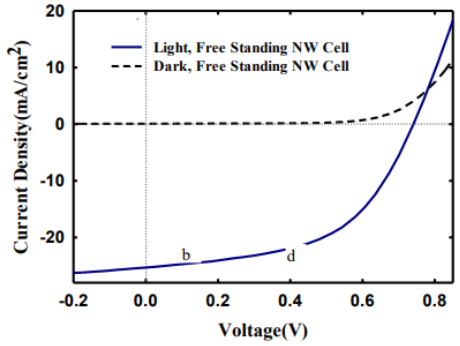

(a)

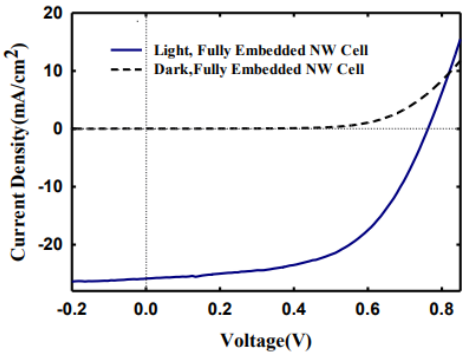

(b)

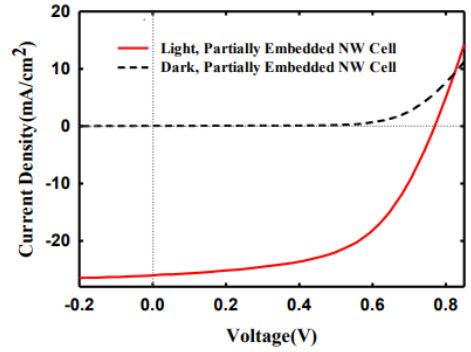

(c)

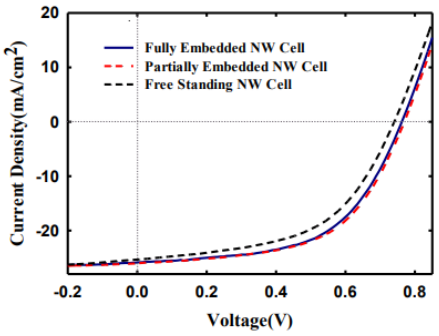

(d)

Figure 3: (a)nanowire solar cells without a substrate, (b)nanowire solar cells with a full substrate embed, and (c)nanowire solar cells with a partial substrate embed. (d) A comparative A comparative J-V analysis of three types of geodesic nanowire solar cells architectures.

Partially integrated nanowire solar cells exhibit an 11.29% power conversion efficiency when exposed to 100 mW/cm2 of solar radiation. The fill factor is 57.1%, the open circuit voltage is 764 mV, and the short current density is 24.9 mA/cm2. With a Voc of 762mV, a fill factor of 56.5%, a power conversion efficiency of 11.09%, and a Jsc of 25.85mA/cm2, the fully integrated nanowire solar cells perform well. With a Jsc of 25.3mA/cm2, Voc of 738mV, and fill factor of 53%, freestanding nanowire solar cells convert electricity at a dismal 9.9 percent efficiency. The effect of design on device performance may be investigated via comparison.

Table 1: Figures indicate the photovoltaic Three solar cells' efficiency in light of geometric nanowires

Structure	n	Jo(A/cm^2)	J_{sc}(mA/cm^2)	V_{oc} (mV)	FF(%)	Efficiency (%)	Rs(Ω /cm^2)	Shunt Resistance (Ω /cm^2)
PENSC	2.50	6.32*10^{-8}	25.9	764	57.1	11.29	4.46	286
FENSC	2.53	6.45*10^{-8}	25.85	762	56.5	11.09	4.47	272
FSNSC	2.79	1.19*10^{-7}	25.3	738	53	9.9	4.86	219

Illustrations Discusses three different nanowire solar cell designs and their corresponding mechanisms for window layer mechanics, electron transport, and hole segregation and movement. More than 25mA/cm2 of brief current is produced by three gematric nanowire solar cells. Air or a translucent AAO membrane account for 68% of the window layer, while the remaining 32% is comprised of CdS nanowires, which contribute significantly to the high Jsc. As a result of the CdS nanowire window layer, external light is better transferred to the CdTe. Three geometric CdS nanowires had very similar transmission spectra, lending credence to this discovery. The transmission spectra of three geometrically distinct CdS nanowires show striking

similarities, showing that almost identical photoexcited carriers are generated in CdTe.

Jsc will be negatively impacted if the interface and bulk are inefficient carrier transporters. It was discovered that individual CdS nanowires only make contact with CdTe at their tips, and that the rest of the window layer is either an AAO membrane or air. Due to the small size (20 nm) of the CdS nanowires and the fact that the CdTe crystals contact both the top and the upper and side surfaces of both CdS nanowires, a junction is formed. The 80 nm long CdS nanowires that come into contact with the CdTe crystal are supported by the AAO membrane.

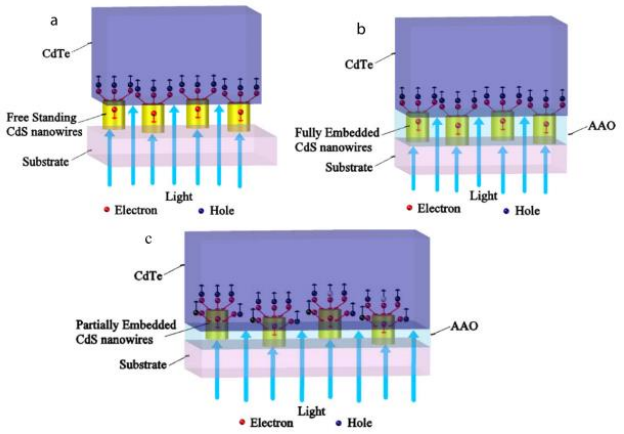

Figure 4: Carrier generation and transport are shown schematically in a, b, and c for nanowire solar cells that are either a) free standing or b) completely embedded or c) partly embedded.

The interface defects and traps in free-standing nanowire solar cells are exacerbated by the exposure of the CdTe above the CdTe-air contact to the external ambient. Possible oxygen and water vapor permeability in the CdS nanowire/CdTe interface. Oxidation develops as a consequence, guiding the growth of traps and interface defects that obstruct carrier transport. As a consequence, this causes an increase in N and Jo while decreasing Jsc and Voc. Micro junctions are formed when CdTe tentacles make touch with SnO2, thanks to the shunting channels provided by the CdTe-Air interface. The weak Voc is due to the 219/cm2 shunting resistance of the free-standing nanowire solar cells. Flaws in the interface, or "traps," caused by moisture and oxygen may be mitigated by maintaining the AAO membrane's incorporation into the glazing system. The inflammatory property of the AAO membrane also inhibits the formation of the CdTe-SnO2 micro connection. The photovoltaic performance of the devices is thereby significantly improved, and their efficiency is increased to well over 11%.

The efficiency of nanowire solar cells that are just partially submerged is somewhat higher than that of completely submerged cells. Growth differences on the nanoscale scale are expected in completely implanted nanowire solar cells due to imperfections and uneven nanowire structural development. Contact between CdTe and CdS nanowires is expected, however the existence of gaps increases the interface roughness and generates interface defects, as seen by the increase in N and Jo but the reduction in fill factor.

Combining AAO and 20nm exposure of cadmium selenide nanowires prevents the partial elimination of CdS nanowires, which would otherwise expose CdTe to the atmosphere. Furthermore, most electron-hole pairs are formed in the axial direction as a result of the interaction between the AAO membrane with CdTe on top and CdS nanowires, whereas only a small number are formed in the lateral direction. Carrier formation and accumulation have been bolstered. The result is anticipated to be an 11.3% rise in production. From what can be seen in SEM photos, photoexcited electrons have an extra 50 nm to traverse across AAO and air before they reach the CdS nanowires. Because of the greater separation, more resistance can be applied. There is worry that excessive series resistance will emerge due to the increased transit time. The micrometer-sized CdTe depletion region absorbs light, as has been explained.

The intense electrical field in the CdTe depletion zone may quickly drift carriers to opposite sides, where they can congregate. When the distance between components is extended by 50 nm, which is much less than a micrometer, the series resistance rises very marginally by a few percent. While the CdTe film and back contacts are responsible for the high series resistance, the graphite paste utilized to construct the back connections in our lab has a sheet resistance of 1200-2400/sql. Future studies will delve further into the supplemental hindrance.

CONCLUSION

On glass-ITO-SnO2 substrates, we generated 100 nm long CdS nanowires that were perfectly aligned and could be entirely embedded in the host AAO membrane, partly embedded in the membrane, or used independently. For CdS-CdTe solar cells, these nanowire layers serve as windows. In order to learn how the AAO membrane impacts solar cell performance, three device configurations were tested. They all showed almost similar transmittance spectra, which proves that the AAO membrane absorbs almost little light and that the same quantity of photons reaches the CdTe absorber layer in each instance. However, the three device arrangements varied in their power conversion efficiency. Nanowire solar cells performed at 9.9%, 11.1%, and 11.3% efficiency when freestanding, completely embedded, and partially embedded, respectively. The electrical performance differences show that the CdTe-AAO interface is superior to the CdTe-air interface due to (i) the passivation of the surface of CdTe, which reduces the density of interface states and traps and enhances electron mobility, and (ii) the elimination of CdTe tentacles that extend down to the tin oxide substrate and cause micro-shunts. PENSCs also have a tiny wrap-around CdS-CdTe junction, which

results in a somewhat higher photocurrent. We have shown that the CdS-CdTe solar cell benefits from both mechanical stability and improved electro-optical properties when the host AAO membrane is kept as a structural component.

REFERENCES

1. Abdelilah Slaoui et.al "Nanomaterials for Photovoltaic Conversion"2020
2. Gerrit Boschloo et.al "Improving the Performance of Dye-Sensitized Solar Cells"
3. Karwan Wasman Qadir "A simulation study on the effect of size gold nanoparticles on broadband light absorption in dye-sensitised solar cells"
4. William Ghann et.al "Dendrimer-based Nanoparticle for Dye Sensitized Solar Cells with Improved Efficiency" DOI: 10.4172/2157-7439.1000496
5. Riya Datta et.al **"**A review on Semiconductor nanoparticles in Photovoltaic cells" International Journal of Advanced Scientific Research and Management, Volume 4 Issue 4, April 2019
6. Olkhovets, R. C. Hsu, A. Lipovskii, and F. W. Wise, Size-Dependent Temperature Variation of the Energy Gap in Lead-Salt Quantum Dots, Phys. Rev. Lett. 81, 3539, 1998.
7. R. Hyun et al. Role of solvent dielectric properties on charge transfer from PbS nanocrystals to molecules. Nano Lett. 10, 318, 2010.
8. Ekimov et al. Absorption and intensity-dependent photoluminescence measurements on CdSe quantum dots: assignment of the first electronic transitions, J. Opt. Soc. Am. B 10, 100, 1993.
9. S. E. Kohn, P. Y. Yu, Y. Petroff, Y. R. Shen, Y. Tsang and M. L. Cohen M L, Electronic Band Structure and Optical Properties of PbTe, PbSe, and PbS, Phys. Rev. B 8, 1477, 1973. See figure 12 and subsequent discussions as well as to a list of such higher energy excitonic transitions in lead salts mentioned in Table 1.
10. J. W. Luo, A. Franceschetti and A. Zunger, Carrier multiplication in semiconductor nanocrystals: theoretical screening of candidate materials based on band-structure effects, Nano lett. 8, 3174, 2008.
11. M. S. Hybertsen, Absorption and emission of light in nanoscale silicon structures, Phys. Rev. Lett. 72, 1514, 1994.; C. Delerue, G. Allan and M. Lannoo, Theoretical aspect of luminescence of porous Si, Phys. Rev. B 48, 11024, 1993.
12. 3 Y. Wang, A. Suna, W. Mahler and R. Kasowski, PbS in polymers from molecules to solids. J. Chem. Phys. 87, 7315, 1987.
13. S. Schmitt-Rink, D. A. B. Miller and D. S. Chemla, Theory of the linear and nonlinear optical properties of semiconductor microcrystallites, Phys Rev. B 35, 8113, 1987. Refer to equation 19.
14. Kamat P V and Meisel D (eds) 1997 Semiconductor Nanoclusters-Physical, Chemical and Catalytic Aspects, Studies in Surface Science and Catalysis series vol. 103, Elsevier, Amsterdam
15. Nazeeruddin Md. K, Kay A, Rodicio I, Humphry-Baker R, MOiler E, Liska P, Vlachopoulos N and Griitzel M 1993 J. Am. Chem. Soc., 115 6382

Corresponding Author

Narendra Kumar*

Research Scholar, S.K.M. University, Dumka